

Supporting Information for “Modeling surface ocean phytoplankton pigments from hyperspectral remote sensing reflectance on global scales”

Sasha J. Kramer^{1,2}, David A. Siegel¹, Stéphane Maritorena¹, Dylan Catlett^{1,2,†}

¹Earth Research Institute, University of California Santa Barbara, Santa Barbara CA, USA.

²Interdepartmental Graduate Program in Marine Science, University of California Santa Barbara, Santa Barbara CA, USA.

† Present address: Biology Department, Woods Hole Oceanographic Institution, Woods Hole, MA, USA.

The Supporting Information presented in this section includes:

Section S1: Supplemental information for the datasets and principal components regression models presented in the main section of the manuscript. This section includes: the results of an Empirical Orthogonal Function (EOF) analysis performed with both the measured and modeled pigment datasets; Pearson’s correlation coefficients between the remote sensing reflectance residual ($\delta R_{rs}(\lambda)$) and each accessory pigment; and the mean model coefficients resulting from the principal components regression modeling.

Section S2: This section includes the results of repeating the principal components regression modeling approach using the first and second derivatives of the measured remote sensing reflectance ($R_{rs,meas}'(\lambda)$ and $R_{rs,meas}''(\lambda)$) instead of the second derivative of the reflectance residual ($\delta R_{rs}''(\lambda)$).

Section S3: This section includes the results of repeating the principal components regression modeling approach using the second derivative of the reflectance residual ($\delta R_{rs}''(\lambda)$) at **5 nm resolution**.

Section S4: This section includes the results of the principal components regression modeling approach using the second derivative of the reflectance residual ($\delta R_{rs}''(\lambda)$) at **10 nm resolution**.

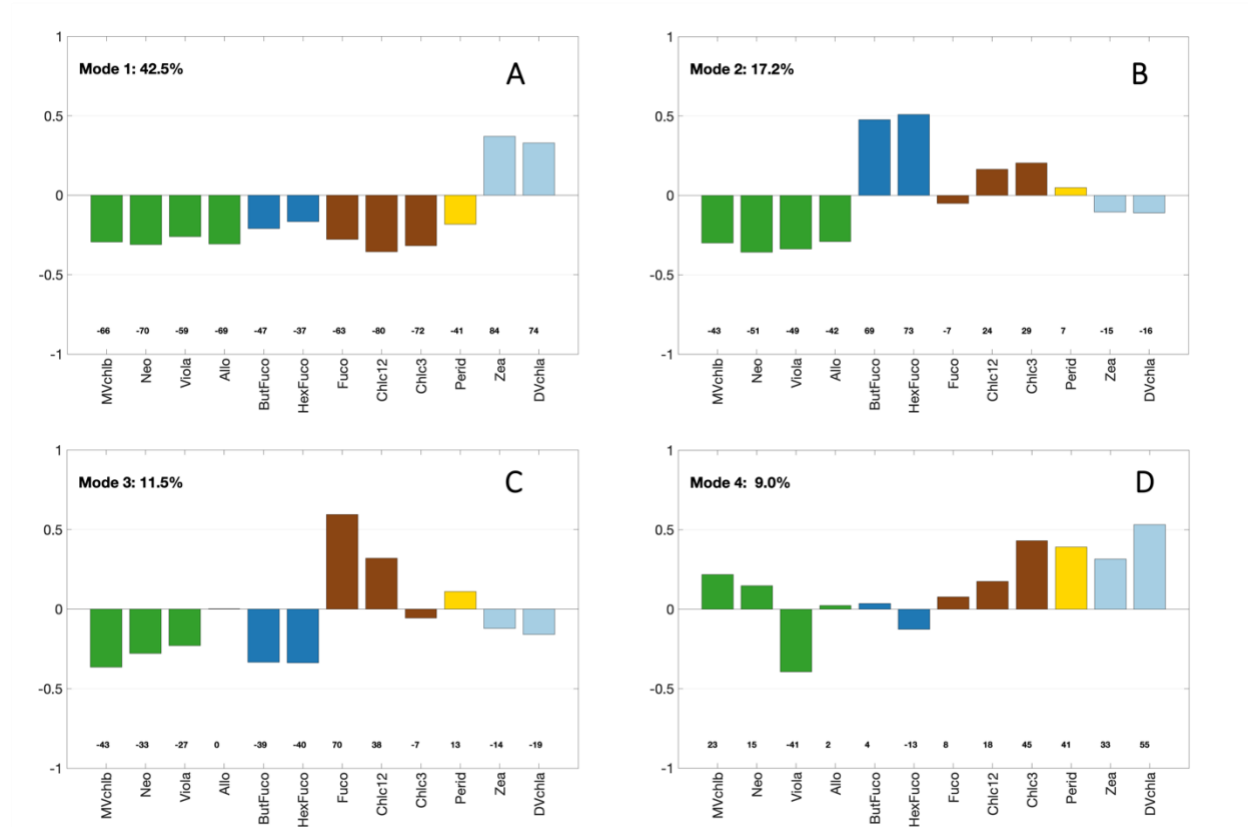
Section S5: This section includes the results of repeating the principal components regression modeling approach using the first and second derivatives of the measured remote sensing reflectance ($R_{rs,meas}'(\lambda)$ and $R_{rs,meas}''(\lambda)$) at **5 nm resolution**.

Section S6: This section includes the results of the principal components regression modeling approach using the first and second derivatives of the measured remote sensing reflectance ($R_{rs,meas}'(\lambda)$ and $R_{rs,meas}''(\lambda)$) at **10 nm resolution**.

Section S7: A and B coefficients in the phytoplankton absorption component of $R_{rs,mod}(\lambda)$.

Section S1

This section addresses additional analysis for the measured and modeled datasets presented in the main manuscript. First, the results of the EOF analysis performed on both the measured (Figure S1A-D) and principal components regression modeled (Figure S1E-H) are shown. The correlations between $\delta R_{rs}(\lambda)$, $\delta R_{rs}'(\lambda)$, and $\delta R_{rs}''(\lambda)$ with the accessory pigments for dinoflagellates, haptophytes, and green algae are also shown (Figures S2-S4). Finally, the median spectral albedo coefficients ($A(\lambda_i)$) optimized across 100-fold cross-validations of the principal components regression models are displayed for each major group of accessory pigments.



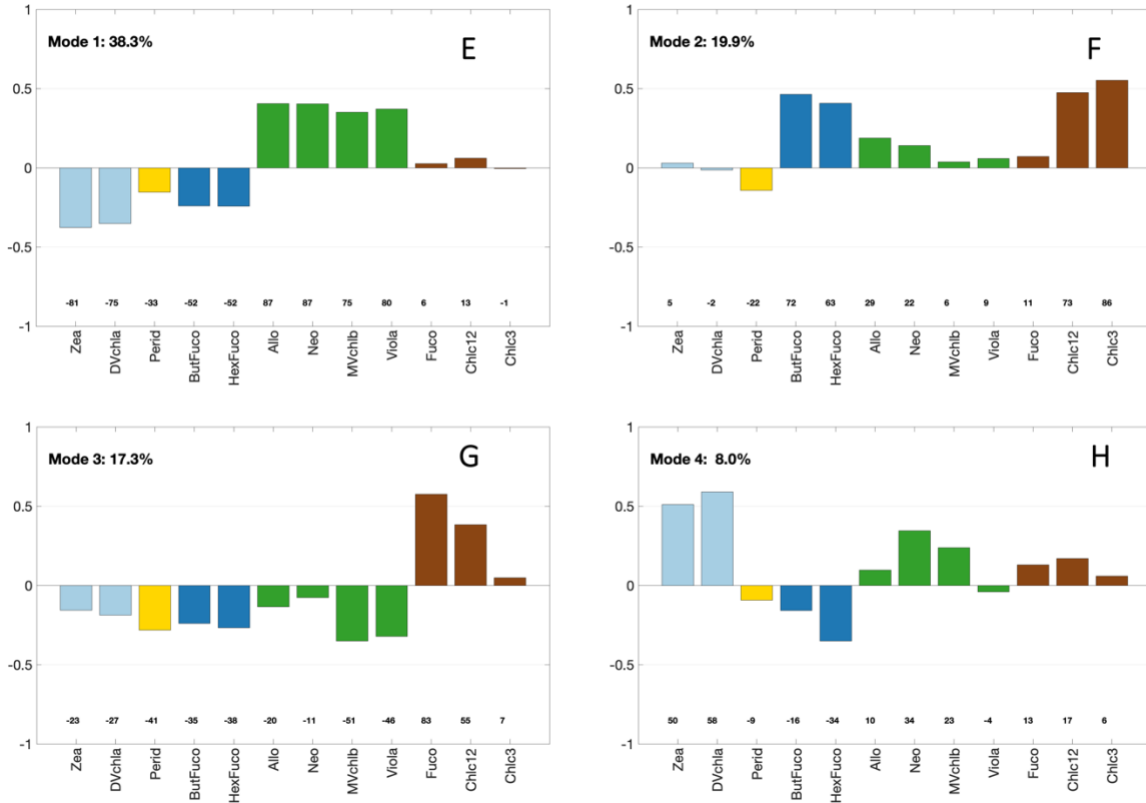


Figure S1. Empirical orthogonal function loadings for measured (A-D) and modeled (E-H) pigments. Modes (A & E) 1, (B & F) 2, (C & G) 3, and (D & H) 4 are displayed for phytoplankton pigment ratios to total chlorophyll-*a*. Loadings are colored based on pigment

clusters (Figure 3): light blue (cyanobacteria), dark blue (haptophytes), green (green algae), brown (diatoms), and gold (dinoflagellates).

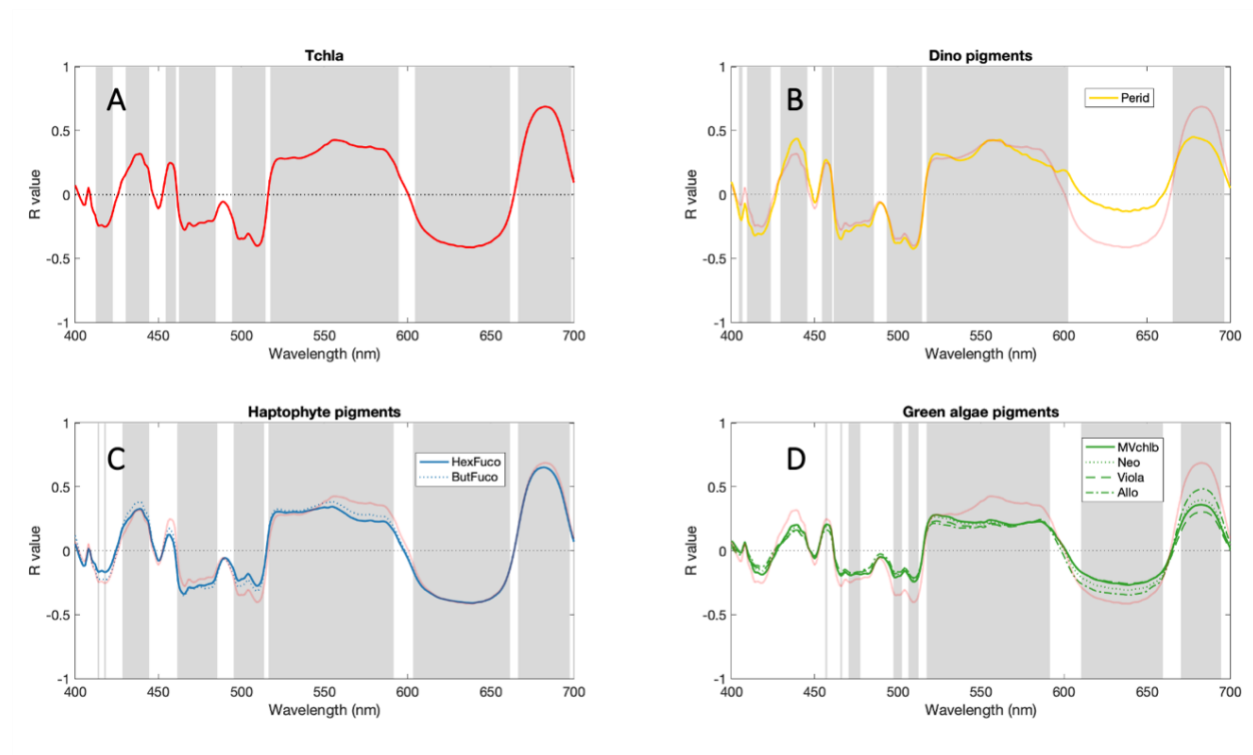


Figure S2. Pearson's correlation coefficients (R) between $\delta R_{rs}(\lambda)$ spectra and pigments, grouped based on the results of hierarchical cluster analysis (Figure 3): (A) Tchla, (B) dinoflagellate pigments, (C) haptophyte pigments, (D) green algal pigments. Grey bars indicate

wavelengths at which the correlation coefficients for all pigments are significantly different from zero.

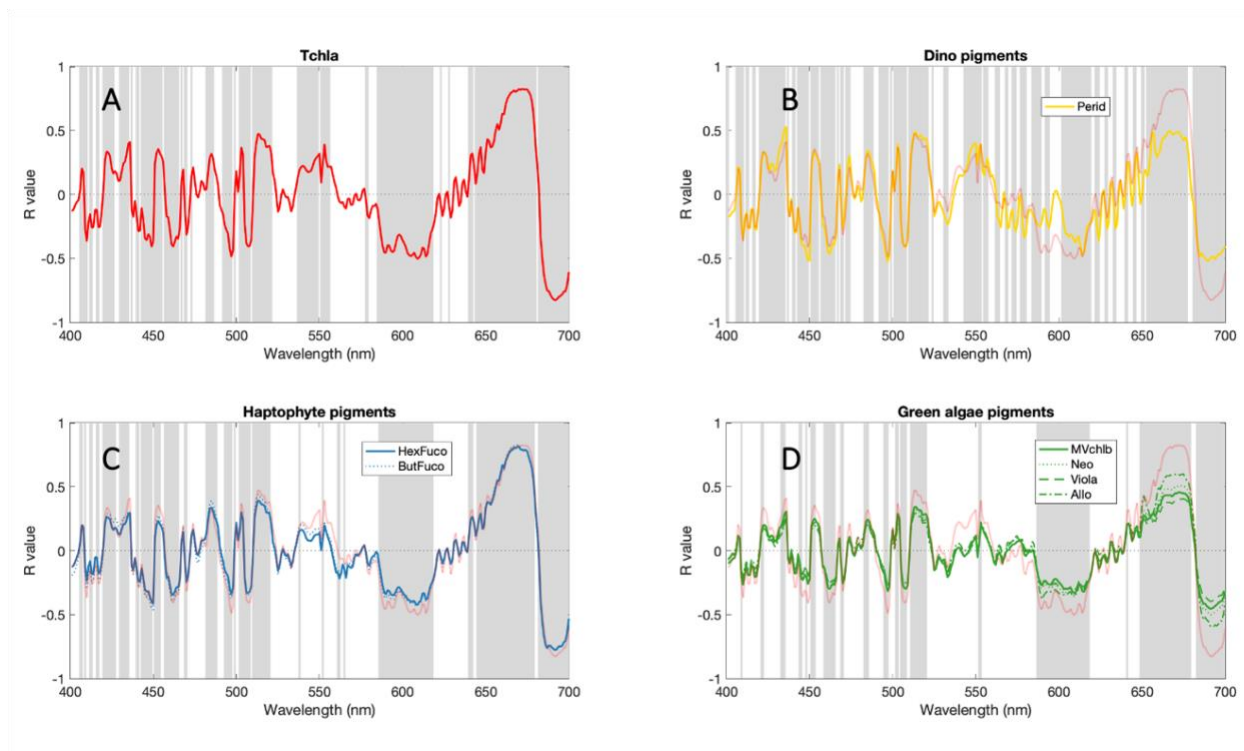


Figure S3. Pearson's correlation coefficients (R) between $\delta R_{rs}'(\lambda)$ spectra and pigments, grouped based on the results of hierarchical cluster analysis (Figure 3): (A) Tchla, (B) dinoflagellate pigments, (C) haptophyte pigments, (D) green algal pigments. Grey bars indicate

wavelengths at which the correlation coefficients for all pigments are significantly different from zero.

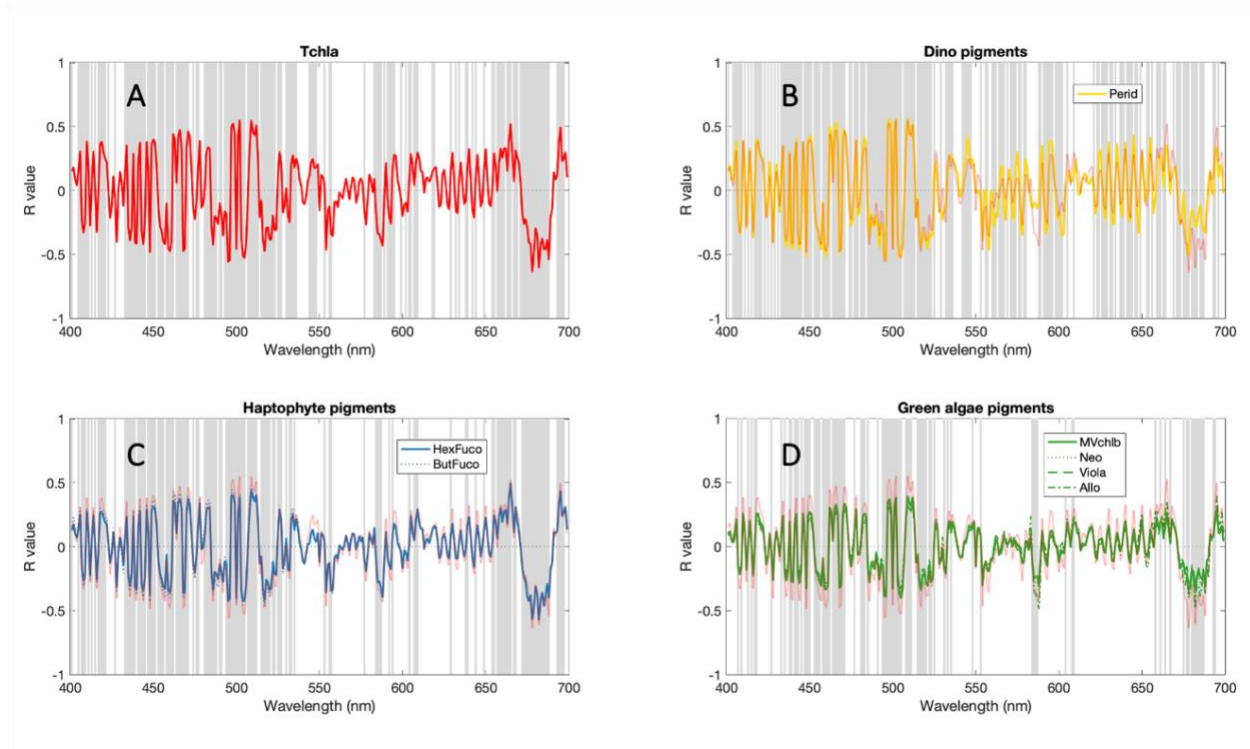


Figure S4. Pearson's correlation coefficients (R) between $\delta R_{rs}(\lambda)$ spectra and pigments, grouped based on the results of hierarchical cluster analysis (Figure 3): (A) Tchla, (B) dinoflagellate pigments, (C) haptophyte pigments, (D) green algal pigments. Grey bars indicate

wavelengths at which the correlation coefficients for all pigments are significantly different from zero.

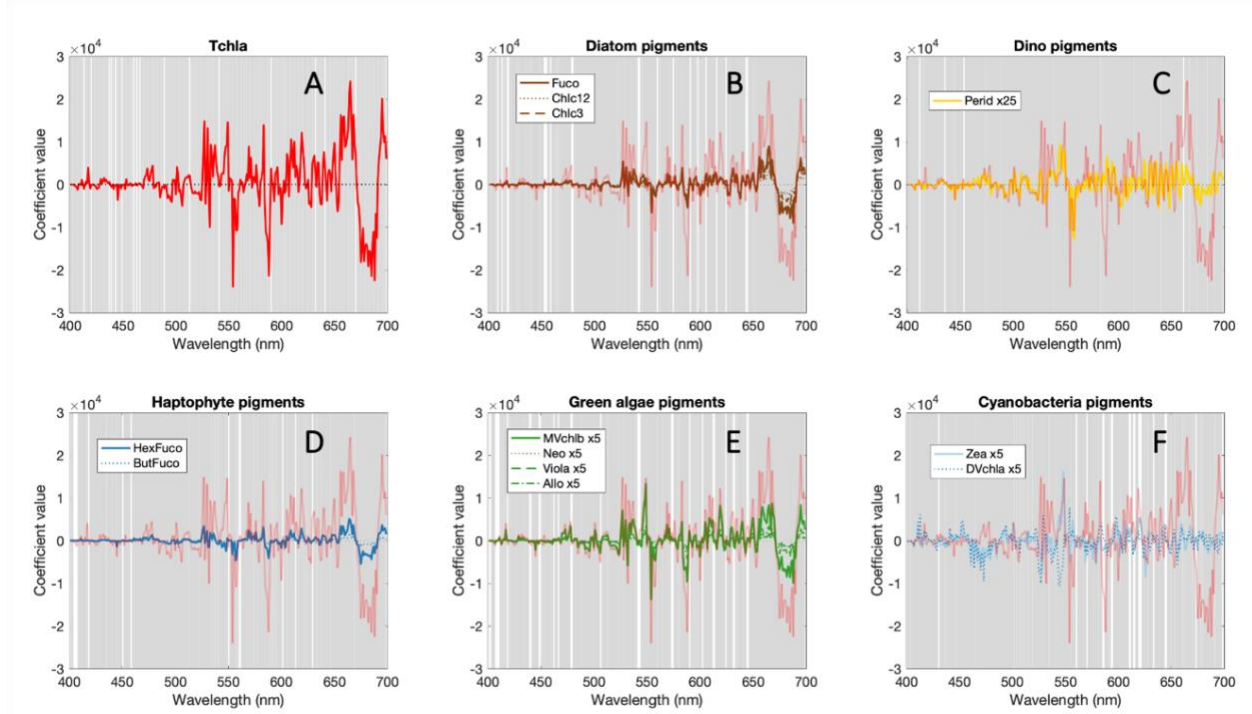


Figure S5. Median model coefficients for all pigments, grouped based on the results of hierarchical cluster analysis (Figure 3): (A) Tchla, (B) diatom pigments, (C) dinoflagellate pigments, (D) haptophyte pigments, (E) green algal pigments, and (F) cyanobacterial pigments. Grey bars indicate wavelengths at which the correlation coefficients for all pigments are significantly different from zero.

Section S2

This section repeats the principal component regression modeling approach presented in the main manuscript, but using $R_{rs,meas}'(\lambda)$ and $R_{rs,meas}''(\lambda)$ as the input rather than $\delta R_{rs}''(\lambda)$:

$$\hat{p}_m = \sum_{i=1}^N A_m(\lambda_i) * R_{rs,meas}'(\lambda_i) + B_i(\lambda_i) * R_{rs,meas}''(\lambda_i) + C_m \text{ [S1].}$$

where $A_m(\lambda_i)$ and $B_m(\lambda_i)$ are the wavelength-specific coefficient applied to $R_{rs,meas}'(\lambda_i)$ and $R_{rs,meas}''(\lambda_i)$, respectively, at the i th wavelengths (λ) for a given pigment concentration (\hat{p}_m), and C_m is an intercept.

All other model parameters were kept exactly the same. The results presented here show the $R_{rs,meas}'(\lambda)$ and $R_{rs,meas}''(\lambda)$ model performance summary (Table S1), the outcome of a hierarchical cluster analysis performed with ratios of modeled accessory pigments to modeled Tchla (Figure S6), an EOF analysis with the ratios of modeled pigments to modeled Tchla

(Figure S7), and correlations between measured and modeled pigment concentrations for Tchl_a and the five major accessory pigments (Figure S8).

Table S1. Summary statistics (R^2 and MAD) and standard deviations of statistics across 100 model cross-validations for all modeled pigments for the $R_{rs,meas}'(\lambda)$ and $R_{rs,meas}''(\lambda)$ model. MAD and its standard deviation are normalized to the mean pigment concentration for each pigment.

Pigment	Mean R^2	SD R^2	Mean normalized MAD	SD normalized MAD
Allo	0.46	0.23	1.296	0.389
But	0.67	0.19	0.544	0.155
Chlc3	0.72	0.15	0.586	0.172
Chlc12	0.76	0.14	0.623	0.188
DVchla	0.55	0.11	0.583	0.103
Fuco	0.73	0.17	0.717	0.232
Hex	0.6	0.2	0.636	0.174
MVchlb	0.44	0.2	0.964	0.306
Neo	0.45	0.22	1.095	0.349
Perid	0.49	0.14	0.779	0.176
Tchl _a	0.75	0.16	0.455	0.104
Viola	0.41	0.19	1.082	0.369
Zea	0.36	0.11	0.465	0.072

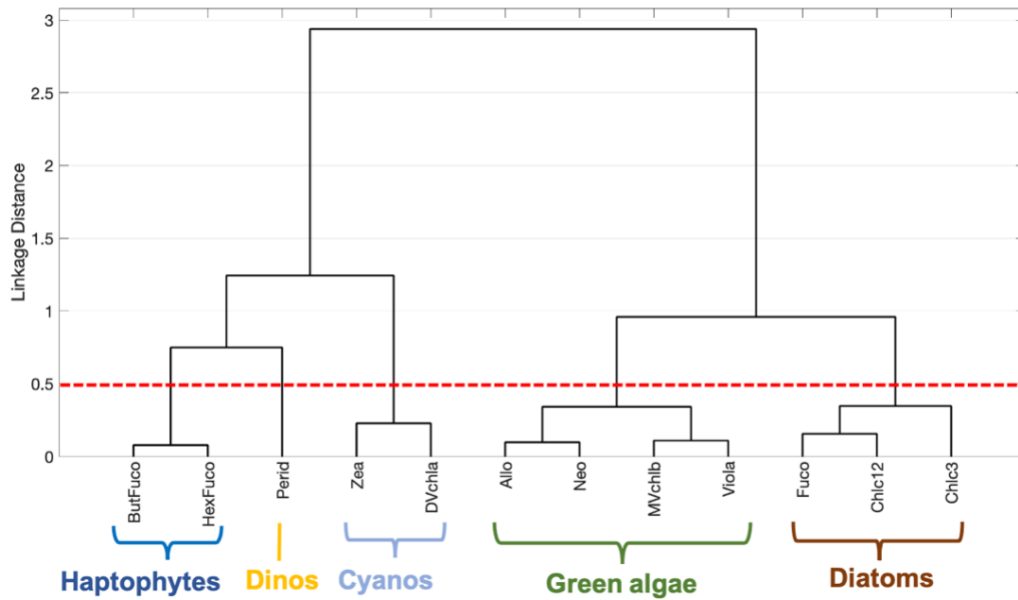


Figure S6. Hierarchical cluster analysis of thirteen modeled pigment ratios to modeled Tchl_a from the $R_{rs,meas}'(\lambda)$ and $R_{rs,meas}''(\lambda)$ model. Using a linkage distance of 0.50 (red dashed

line), five distinct groups emerge: haptophytes (dark blue), diatoms (brown), dinoflagellates (gold), green algae (green), and cyanobacteria (light blue).

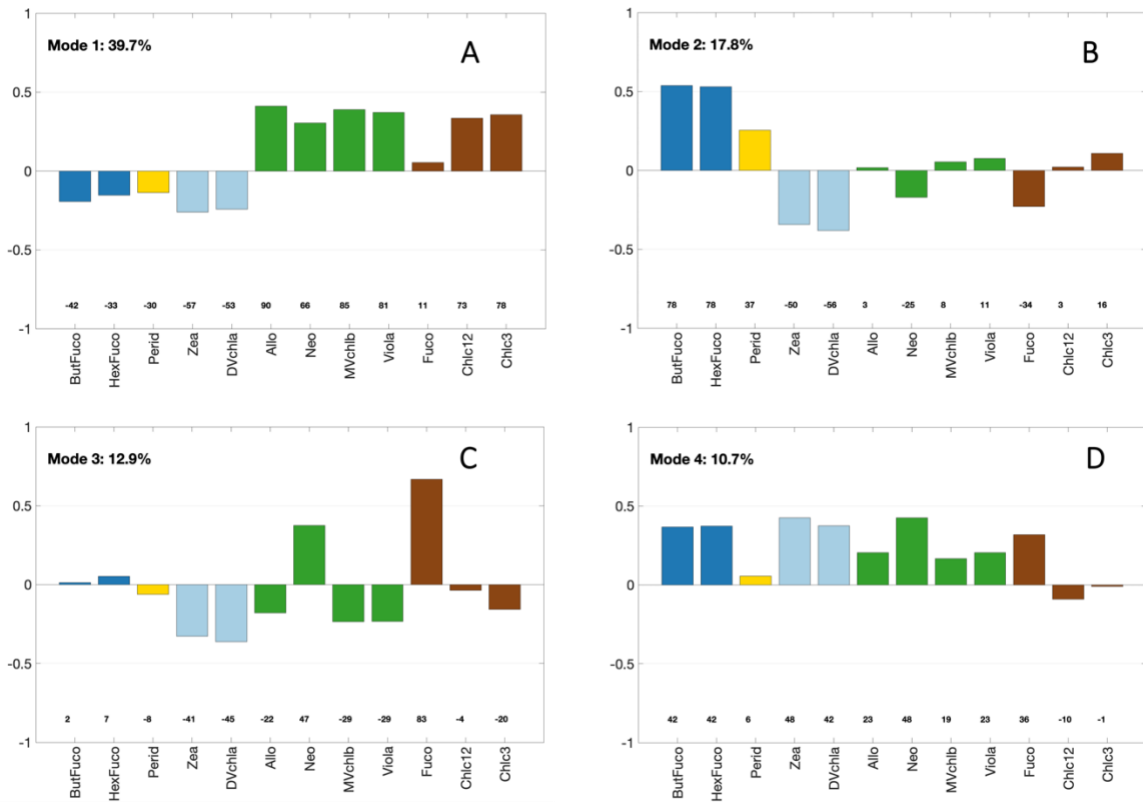


Figure S7. Empirical orthogonal function loadings for the reconstructed pigments of the $R_{rs,meas}'(\lambda)$ and $R_{rs,meas}''(\lambda)$ model. Modes (A) 1, (B) 2, (C) 3, and (D) 4 were calculated for phytoplankton pigment ratios to total chlorophyll-a concentration. Loadings are colored based on

pigment clusters (Figure S6): light blue (cyanobacteria), dark blue (haptophytes), green (green algae), brown (diatoms), and gold (green algae).

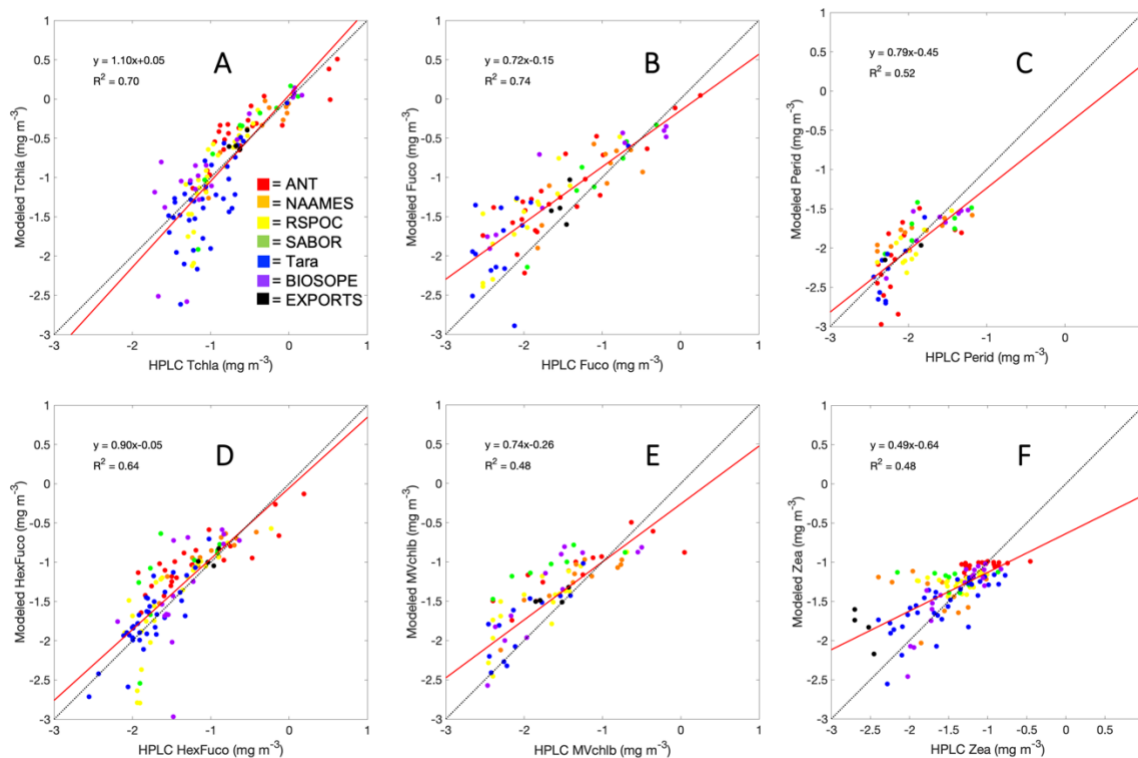


Figure S8. Correlation between HPLC measured pigments and principal components regression modeled pigments using the $R_{rs,meas}'(\lambda)$ and $R_{rs,meas}''(\lambda)$ model: (A) Tchl_a, (B) Fuco, (C) Perid, (D) HexFuco, (E) MVchl_b, (F) Zea. The 1:1 line is shown in black; the linear fit is shown in red. Samples are colored by source (red = ANT, orange = NAAMES, yellow = RemSensPOC [RSPOC], green = SABOR, blue = Tara, purple = BIOSOPE, black = EXPORTS).

Section S3

This section repeats the principal component regression modeling approach presented in the main manuscript, using $\delta R_{rs}''(\lambda)$ at 5nm resolution (every 5nm from 400-700nm). All other model parameters were kept exactly the same. The results presented here show the model performance summary (Table S2), the outcome of a hierarchical cluster analysis performed with ratios of modeled accessory pigments to modeled Tchl_a (Figure S9), an EOF analysis with the ratios of modeled pigments to modeled Tchl_a (Figure S10), and correlations between measured and modeled pigment concentrations for Tchl_a and the five major accessory pigments (Figure S11). Spectral model coefficients are also shown (Figure S12).

Table S2. Summary statistics (R^2 and MAD) and standard deviations of statistics across 100 model cross-validations for all modeled pigments using $\delta R_{rs}''(\lambda)$ at 5nm resolution. MAD and

its standard deviation are normalized to the mean pigment concentration for each pigment.

Pigment	Mean R2	SD R2	Mean normalized MAD	SD normalized MAD
Allo	0.38	0.16	1.329	0.390
But	0.59	0.15	0.613	0.185
Chlc3	0.66	0.12	0.680	0.199
Chlc12	0.66	0.12	0.751	0.229
DVchla	0.42	0.11	0.688	0.111
Fuco	0.63	0.13	0.903	0.261
Hex	0.54	0.16	0.704	0.193
MVchl b	0.41	0.19	0.985	0.305
Neo	0.4	0.19	1.151	0.358
Perid	0.45	0.12	0.825	0.167
Tchla	0.68	0.15	0.532	0.122
Viola	0.36	0.17	1.115	0.385
Zea	0.35	0.11	0.491	0.076

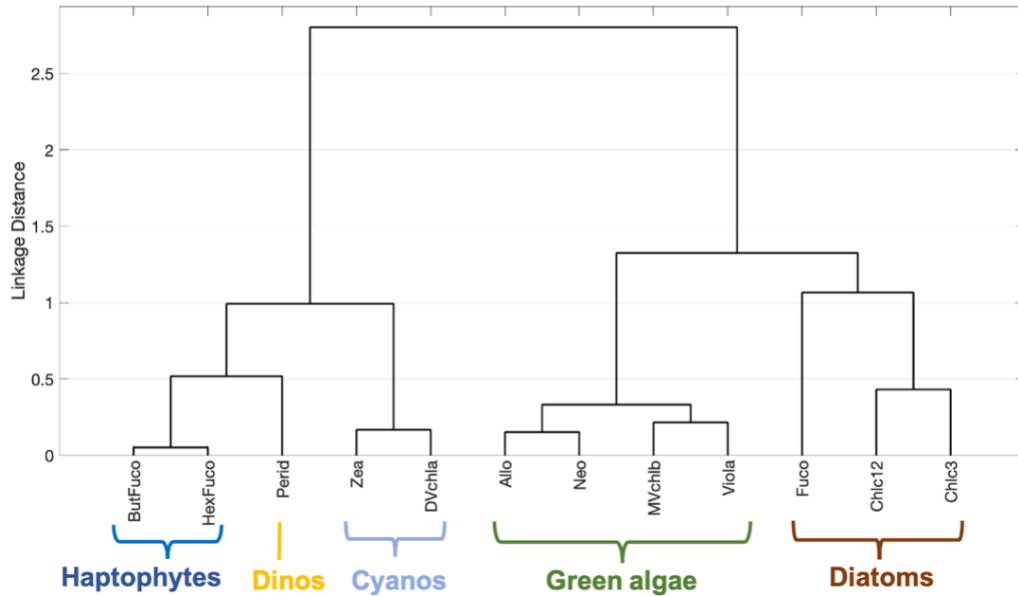


Figure S9. Hierarchical cluster analysis of thirteen modeled pigment ratios to modeled Tchla from the $\delta R_{rs}''(\lambda)$ model at 5 nm resolution. Five distinct groups emerge: haptophytes (dark

blue), diatoms (brown), dinoflagellates (gold), green algae (green), and cyanobacteria (light blue).

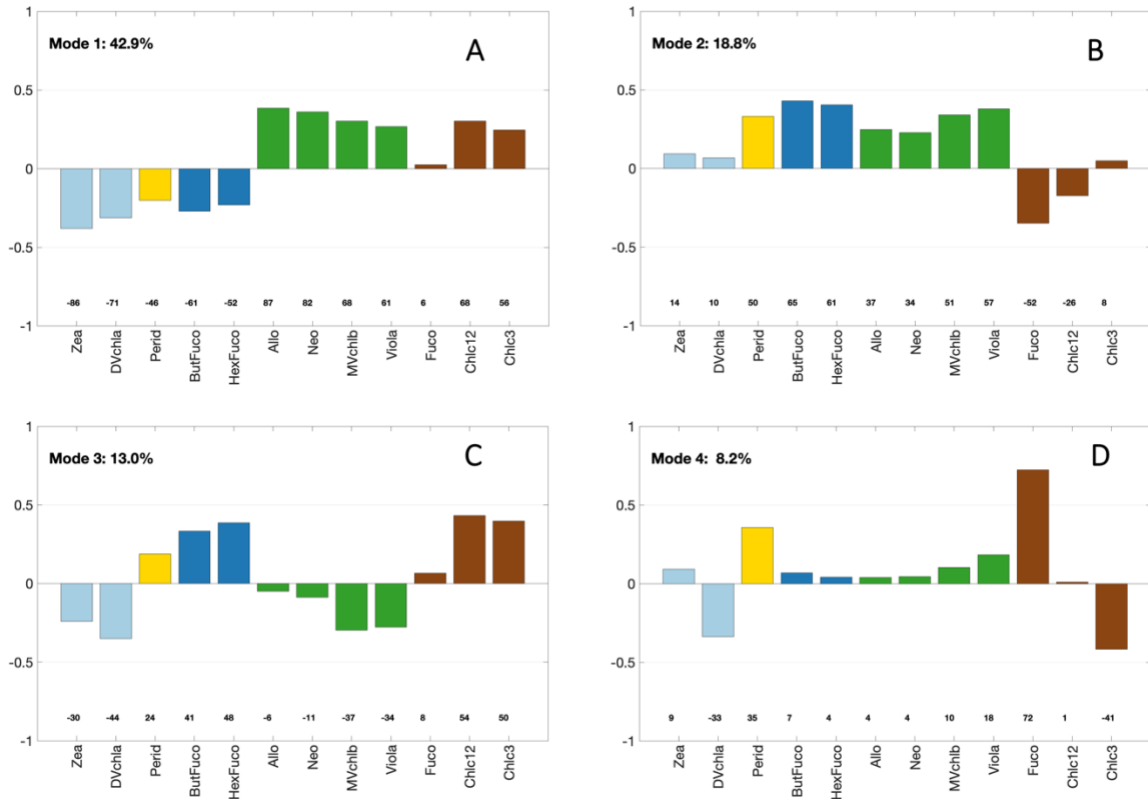


Figure S10. Empirical orthogonal function loadings reconstructed from the $\delta R_{rs}''(\lambda)$ model at 5 nm resolution for Modes (A) 1, (B) 2, (C) 3, and (D) 4, calculated for phytoplankton pigment ratios to total chlorophyll-a concentration. Loadings are colored based on pigment clusters

(Figure S9): light blue (cyanobacteria), dark blue (haptophytes), green (green algae), brown (diatoms), and gold (green algae).

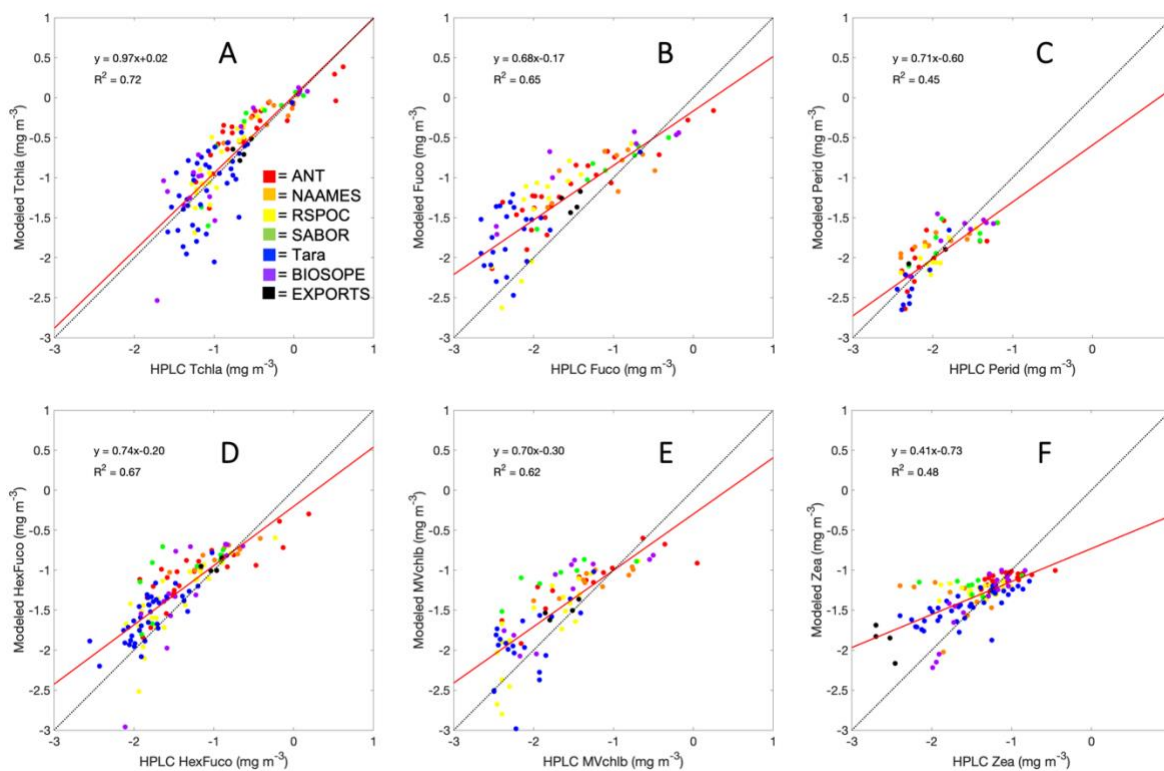


Figure S11. Correlation between HPLC measured pigments and principal components regression modeled pigments constructed from the $\delta R_{rs}''(\lambda)$ model at 5 nm resolution: (A) Tchla, (B) Fuco, (C) Perid, (D) HexFuco, (E) MVchl b, (F) Zea. The 1:1 line is shown in black; the linear fit is shown in red. Samples are colored by source (red = ANT, orange = NAAMES,

yellow = RemSensPOC [RSPOC], green = SABOR, blue = Tara, purple = BIOSOPE, black = EXPORTS).

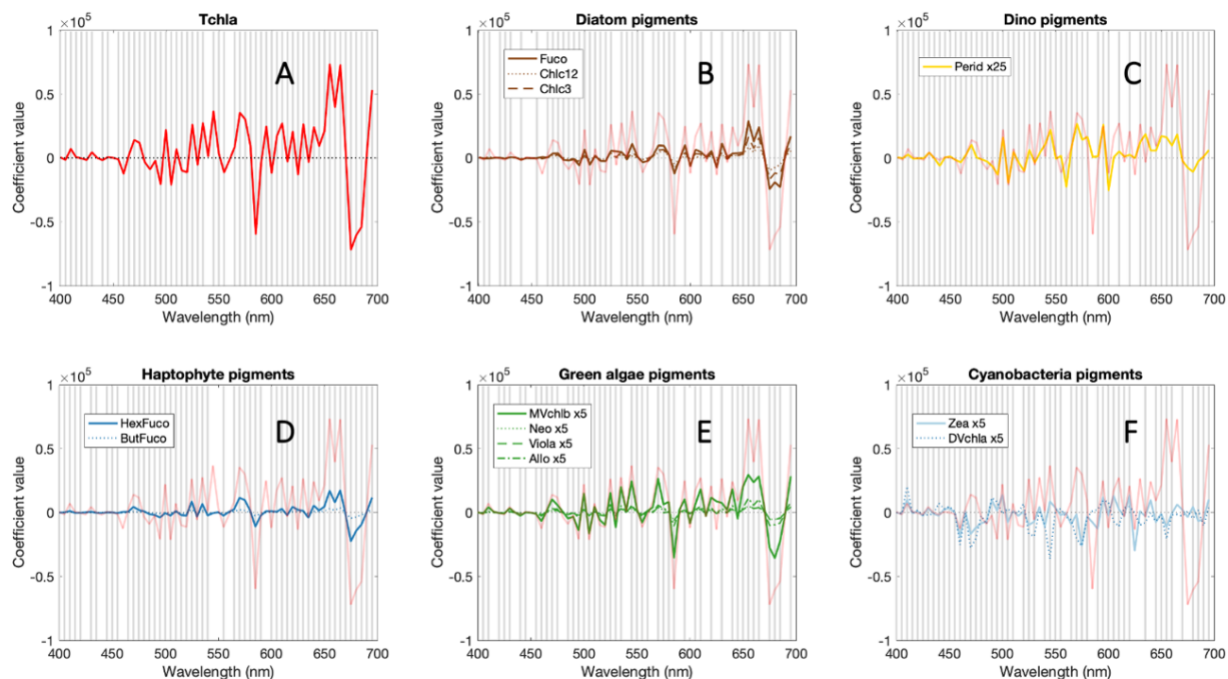


Figure S12. Median model coefficients from the $\delta R_{rs}(\lambda)$ model at 5 nm resolution for all pigments, grouped based on the results of hierarchical cluster analysis (Figure S9): (A) Tchla, (B) diatom pigments, (C) dinoflagellate pigments, (D) haptophyte pigments, (E) green algal pigments, and (F) cyanobacterial pigments. Grey bars indicate wavelengths at which the correlation coefficients for all pigments are significantly different from zero.

Section S3

This section repeats the principal component regression modeling approach presented in the main manuscript (using $\delta R_{rs}(\lambda)$) at 10nm resolution (every 10nm from 400-700nm). All other model parameters were kept exactly the same. Model performance is compared for $\delta R_{rs}(\lambda)$ at 10 nm resolution (Table S3).

Table S3. Summary statistics (R^2 and MAD) and standard deviations of statistics across 100 model cross-validations for all modeled pigments using $\delta R_{rs}(\lambda)$ at 10nm resolution. MAD and

its standard deviation are normalized to the mean pigment concentration for each pigment.

Pigment	Mean R2	SD R2	Mean normalized MAD	SD normalized MAD
Allo	0.27	0.11	1.418	0.392
But	0.42	0.12	0.725	0.183
Chlc3	0.45	0.11	0.841	0.208
Chlc12	0.44	0.13	0.918	0.238
DVchla	0.44	0.11	0.683	0.112
Fuco	0.42	0.11	1.072	0.266
Hex	0.36	0.13	0.808	0.193
MVchl b	0.36	0.16	1.055	0.303
Neo	0.33	0.14	1.271	0.344
Perid	0.43	0.11	0.843	0.166
Tchla	0.52	0.14	0.654	0.133
Viola	0.29	0.13	1.202	0.377
Zea	0.33	0.12	0.490	0.075

Section S4

This section repeats the principal component regression modeling approach presented in Section S2, using $R_{rs,meas}'(\lambda)$ and $R_{rs,meas}''(\lambda)$ at 5nm resolution (every 5nm from 400-700nm). All other model parameters were kept exactly the same. The results presented here show the model performance summary (Table S4), the outcome of a hierarchical cluster analysis performed with ratios of modeled accessory pigments to modeled Tchla (Figure S13), an EOF analysis with the ratios of modeled pigments to modeled Tchla (Figure 14), and correlations between measured and modeled pigment concentrations for Tchla and the five major accessory pigments (Figure 15).

Table S4. Summary statistics (R^2 and MAD) and standard deviations of statistics across 100 model cross-validations for all modeled pigments using $R_{rs,meas}'(\lambda)$ and $R_{rs,meas}''(\lambda)$ at 5nm resolution. MAD and its standard deviation are normalized to the mean pigment concentration

for each pigment.

Pigment	Mean R2	SD R2	Mean normalized MAD	SD normalized MAD
Allo	0.44	0.22	1.247	0.410
But	0.66	0.18	0.557	0.166
Chlc3	0.71	0.15	0.605	0.176
Chlc12	0.73	0.14	0.666	0.196
DVchla	0.5	0.1	0.623	0.104
Fuco	0.71	0.17	0.751	0.224
Hex	0.59	0.19	0.651	0.177
MVchl b	0.44	0.21	0.966	0.307
Neo	0.44	0.22	1.091	0.355
Perid	0.49	0.14	0.785	0.177
Tchla	0.73	0.17	0.475	0.105
Viola	0.4	0.2	1.094	0.375
Zea	0.35	0.11	0.466	0.073

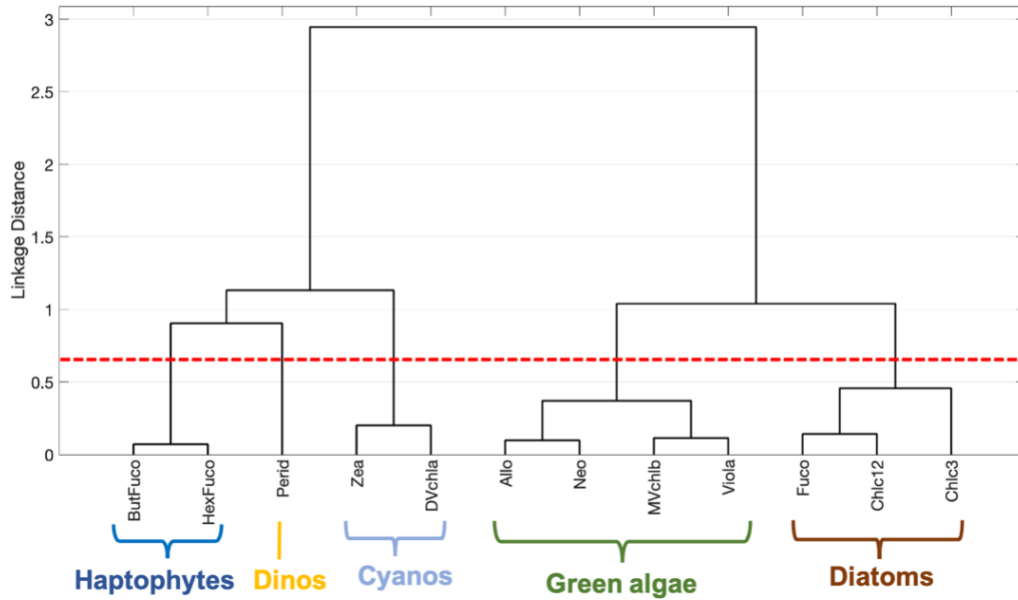


Figure S13. Hierarchical cluster analysis of thirteen modeled pigment ratios to modeled Tchla from the $R_{rs,meas}'(\lambda)$ and $R_{rs,meas}''(\lambda)$ model at 5nm resolution. Using a linkage distance of

0.60 (red dashed line), five distinct groups emerge: haptophytes (dark blue), diatoms (brown), dinoflagellates (gold), green algae (green), and cyanobacteria (light blue).

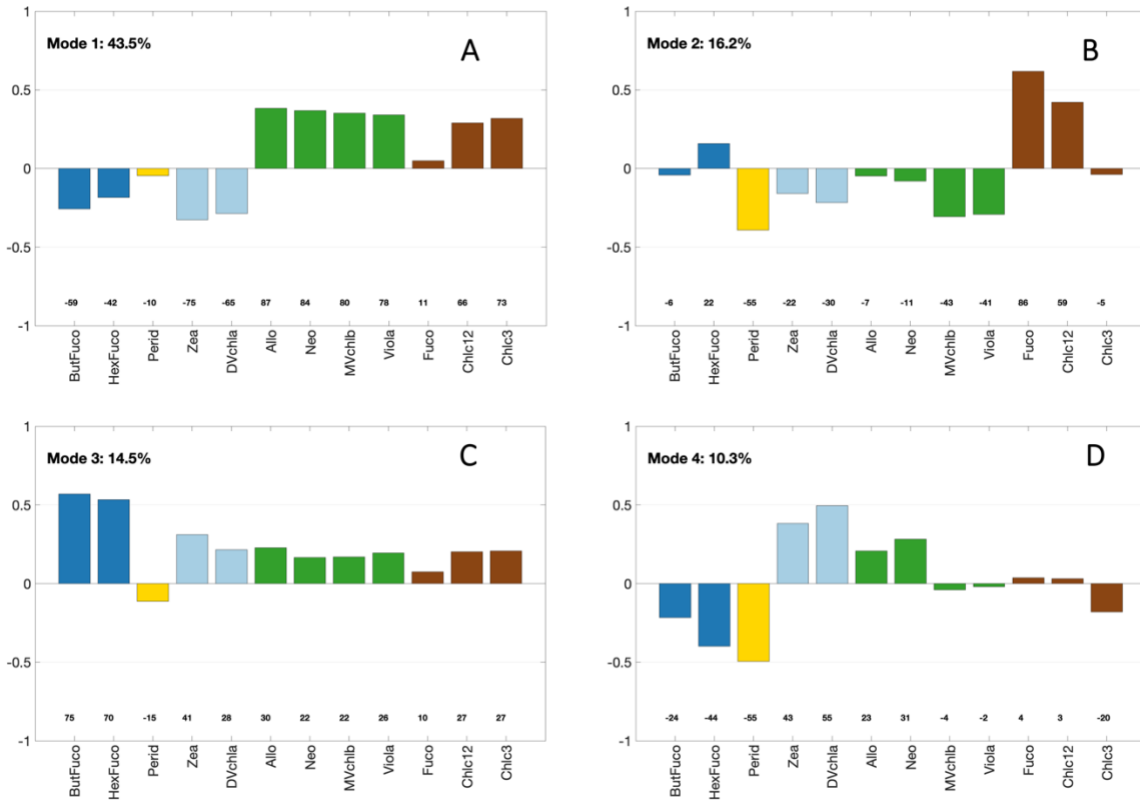


Figure S14. Empirical orthogonal function loadings constructed from the $R_{rs,meas}'(\lambda)$ and $R_{rs,meas}''(\lambda)$ model at 5nm resolution for Modes (A) 1, (B) 2, (C) 3, and (D) 4, calculated for phytoplankton pigment ratios to total chlorophyll-a concentration. Loadings are colored based on

pigment clusters (Figure S13): light blue (cyanobacteria), dark blue (haptophytes), green (green algae), brown (diatoms), and gold (green algae).

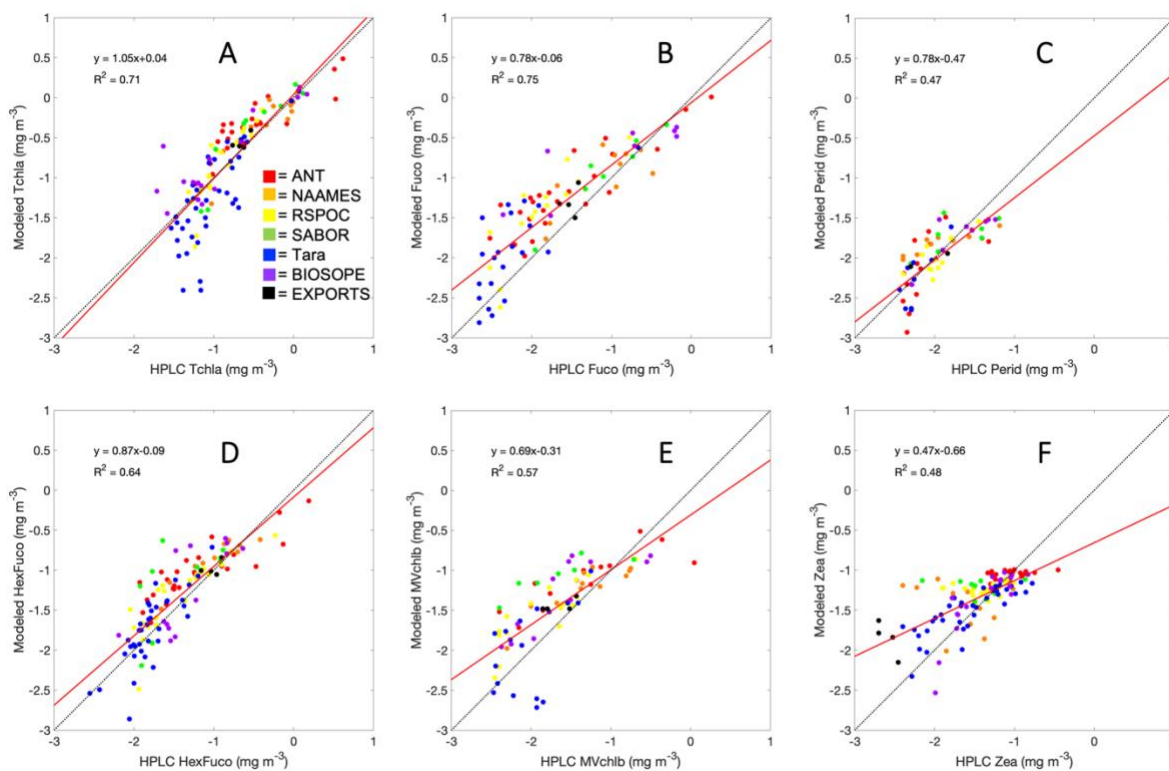


Figure S15. Correlation between HPLC measured pigments and principal components regression modeled pigments from the $R_{rs,meas}'(\lambda)$ and $R_{rs,meas}''(\lambda)$ model at 5nm resolution: (A) Tchla, (B) Fuco, (C) Perid, (D) HexFuco, (E) MVchl b, (F) Zea. The 1:1 line is shown in black; the linear fit is shown in red. Samples are colored by source (red = ANT, orange = NAAMES, yellow = RemSensPOC [RSPOC], green = SABOR, blue = Tara, purple = BIOSOPE, black = EXPORTS).

Section S6

This section repeats the principal component regression modeling approach presented in Section S2 (using $R_{rs,meas}'(\lambda)$ and $R_{rs,meas}''(\lambda)$) at 10nm resolution (every 10nm from 400-700nm). All other model parameters were kept exactly the same. Model performance is compared for $R_{rs,meas}'(\lambda)$ and $R_{rs,meas}''(\lambda)$ at 10 nm resolution (Table S5).

Table S5. Summary statistics (R^2 and MAD) and standard deviations of statistics across 100 model cross-validations for all modeled pigments using $R_{rs,meas}'(\lambda)$ and $R_{rs,meas}''(\lambda)$ at 10nm resolution. MAD and its standard deviation are normalized to the mean pigment concentration

for each pigment.

Pigment	Mean R2	SD R2	Mean normalized MAD	SD normalized MAD
Allo	0.39	0.19	1.331	0.408
But	0.57	0.19	0.617	0.173
Chlc3	0.63	0.17	0.703	0.176
Chlc12	0.65	0.16	0.771	0.197
DVchla	0.5	0.11	0.627	0.105
Fuco	0.65	0.19	0.859	0.225
Hex	0.5	0.18	0.726	0.183
MVchl b	0.42	0.21	0.987	0.315
Neo	0.41	0.22	1.165	0.350
Perid	0.48	0.14	0.808	0.167
Tchla	0.69	0.18	0.534	0.113
Viola	0.39	0.19	1.124	0.380
Zea	0.38	0.11	0.456	0.070

Section S7:

In the reflectance model used here, the phytoplankton absorption component is constructed as a function of chlorophyll: $a_{ph}(\lambda) = A(\lambda) * Tchla^{B(\lambda)}$. The **A** and **B** coefficients used here are shown below in **Table S6**.

Wavelength (λ)	A	B	λ	A	B
400	0.0361528	0.820472	417	0.0450843	0.781304
401	0.0366568	0.817517	418	0.0455743	0.780118
402	0.0371692	0.81458	419	0.0460527	0.779034
403	0.037689	0.811675	420	0.0465182	0.778042
404	0.038215	0.808814	421	0.0469695	0.77713
405	0.0387458	0.806011	422	0.0474052	0.776289
406	0.0392805	0.803279	423	0.047824	0.77551
407	0.0398179	0.80063	424	0.0482245	0.774782
408	0.0403567	0.79808	425	0.0486052	0.774096
409	0.040896	0.795641	426	0.0489645	0.773442
410	0.0414344	0.793327	427	0.0493011	0.772811
411	0.0419709	0.791153	428	0.0496133	0.772193
412	0.0425044	0.789132	429	0.0498994	0.77158
413	0.0430336	0.787276	430	0.0501578	0.77096
414	0.0435575	0.785576	431	0.0503868	0.770326
415	0.0440747	0.784022	432	0.0505845	0.769668
416	0.044584	0.782601	433	0.0507492	0.768975

Wavelength (λ)	A	B	λ	A	B
434	0.0508788	0.76824	471	0.0406587	0.752086
435	0.0509714	0.767451	472	0.0402921	0.752333
436	0.051025	0.7666	473	0.0399081	0.752526
437	0.0510373	0.765675	474	0.0395075	0.752676
438	0.0510062	0.764669	475	0.0390911	0.752799
439	0.0509293	0.763569	476	0.0386597	0.752907
440	0.0508043	0.762366	477	0.0382142	0.753015
441	0.0506286	0.761049	478	0.0377551	0.753135
442	0.0503996	0.759607	479	0.0372833	0.753282
443	0.0501146	0.75803	480	0.0367994	0.753468
444	0.0497729	0.756315	481	0.036304	0.753708
445	0.0493817	0.754497	482	0.0357979	0.754015
446	0.0489503	0.752621	483	0.0352815	0.754403
447	0.0484879	0.750731	484	0.0347555	0.754887
448	0.0480036	0.748871	485	0.0342205	0.75548
449	0.0475065	0.747084	486	0.0336771	0.756197
450	0.0470055	0.745416	487	0.0331256	0.757053
451	0.0465099	0.74391	488	0.0325668	0.758063
452	0.0460285	0.742613	489	0.032001	0.759242
453	0.0455705	0.741568	490	0.0314288	0.760606
454	0.045145	0.740822	491	0.0308507	0.762167
455	0.0447612	0.740421	492	0.0302675	0.76392
456	0.0444255	0.740395	493	0.0296799	0.765857
457	0.044133	0.740704	494	0.0290889	0.767971
458	0.043876	0.741294	495	0.028495	0.770253
459	0.043647	0.742108	496	0.0278993	0.772698
460	0.0434384	0.743092	497	0.0273023	0.775298
461	0.0432427	0.744191	498	0.026705	0.778047
462	0.0430524	0.745351	499	0.026108	0.780938
463	0.0428601	0.746518	500	0.0255122	0.783966
464	0.0426582	0.747638	501	0.0249184	0.787125
465	0.0424394	0.748657	502	0.0243273	0.79041
466	0.0421975	0.749532	503	0.0237396	0.793816
467	0.0419323	0.750265	504	0.0231564	0.797338
468	0.0416447	0.750873	505	0.0225782	0.800971
469	0.0413359	0.75137	506	0.022006	0.804711
470	0.0410069	0.751769	507	0.0214405	0.808554

Wavelength (λ)	A	B	λ	A	B
508	0.0208826	0.812496	545	0.0086346	0.937605
509	0.0203333	0.816533	546	0.0084485	0.939341
510	0.0197932	0.820661	547	0.0082646	0.940989
511	0.0192634	0.824875	548	0.0080827	0.942548
512	0.0187445	0.829159	549	0.0079025	0.944017
513	0.0182373	0.833496	550	0.0077237	0.945396
514	0.0177427	0.837866	551	0.007546	0.946684
515	0.0172614	0.842253	552	0.007369	0.947879
516	0.0167942	0.846638	553	0.007193	0.94898
517	0.0163421	0.851005	554	0.007018	0.949986
518	0.0159059	0.855334	555	0.006842	0.950895
519	0.0154865	0.859608	556	0.006667	0.951707
520	0.015085	0.86381	557	0.006492	0.952428
521	0.0147019	0.867924	558	0.006321	0.953066
522	0.0143363	0.871945	559	0.006153	0.953629
523	0.0139871	0.875875	560	0.00599	0.954124
524	0.0136531	0.879711	561	0.005833	0.954559
525	0.0133332	0.883451	562	0.005685	0.954942
526	0.0130262	0.887096	563	0.005545	0.955279
527	0.0127311	0.890643	564	0.005416	0.955578
528	0.0124468	0.89409	565	0.005299	0.955845
529	0.0121722	0.897435	566	0.005195	0.956087
530	0.0119064	0.900676	567	0.005103	0.956307
531	0.0116484	0.903812	568	0.005024	0.956508
532	0.0113978	0.906843	569	0.004955	0.95669
533	0.0111541	0.909774	570	0.004897	0.956857
534	0.0109168	0.912604	571	0.004848	0.95701
535	0.0106857	0.915338	572	0.004809	0.957151
536	0.0104604	0.917975	573	0.004778	0.957283
537	0.0102404	0.920519	574	0.004754	0.957407
538	0.0100255	0.92297	575	0.004737	0.957525
539	0.0098153	0.925329	576	0.004727	0.95764
540	0.0096094	0.927598	577	0.004723	0.957753
541	0.0094076	0.929777	578	0.004724	0.957867
542	0.0092095	0.931866	579	0.00473	0.957982
543	0.0090149	0.933868	580	0.00474	0.958101
544	0.0088233	0.935781	581	0.004753	0.958227

Wavelength (λ)	A	B	λ	A	B
582	0.004769	0.958361	619	0.005635	0.972645
583	0.004788	0.958504	620	0.005698	0.972999
584	0.004808	0.95866	621	0.005766	0.973331
585	0.00483	0.95883	622	0.00584	0.973638
586	0.004853	0.959015	623	0.00592	0.973919
587	0.004876	0.95922	624	0.006006	0.974172
588	0.004899	0.959444	625	0.006099	0.974394
589	0.004921	0.959691	626	0.006199	0.974584
590	0.004942	0.959963	627	0.006305	0.974744
591	0.004961	0.960261	628	0.006418	0.974873
592	0.004978	0.960584	629	0.006537	0.974974
593	0.004994	0.960931	630	0.006663	0.975048
594	0.005009	0.961299	631	0.006793	0.975095
595	0.005023	0.961686	632	0.00693	0.975118
596	0.005036	0.962092	633	0.007071	0.975115
597	0.005049	0.962513	634	0.007218	0.97509
598	0.005061	0.962949	635	0.007369	0.975042
599	0.005073	0.963398	636	0.007525	0.974973
600	0.005085	0.963858	637	0.007685	0.974883
601	0.005098	0.964328	638	0.007849	0.974773
602	0.005111	0.964805	639	0.008017	0.974645
603	0.005125	0.965289	640	0.008189	0.974497
604	0.00514	0.965778	641	0.008365	0.974332
605	0.005156	0.96627	642	0.008544	0.97415
606	0.005173	0.966765	643	0.008727	0.973951
607	0.005192	0.967259	644	0.008912	0.973736
608	0.005213	0.967752	645	0.009101	0.973506
609	0.005236	0.968242	646	0.009293	0.973261
610	0.005261	0.968728	647	0.009488	0.973001
611	0.005289	0.969208	648	0.009685	0.972728
612	0.00532	0.969681	649	0.009885	0.972441
613	0.005354	0.970144	650	0.010087	0.97214
614	0.005391	0.970597	651	0.010292	0.971827
615	0.005431	0.971038	652	0.010499	0.971501
616	0.005476	0.971465	653	0.010708	0.971163
617	0.005524	0.971876	654	0.010919	0.970813
618	0.005578	0.97227	655	0.011133	0.970451

Wavelength (λ)	A	B	λ	A	B
656	0.011348	0.970078	693	0.008581	1.027931
657	0.011565	0.969693	694	0.007726	1.034717
658	0.011784	0.969298	695	0.006829	1.041786
659	0.012004	0.968892	696	0.005891	1.049128
660	0.012227	0.968475	697	0.004914	1.056734
661	0.012451	0.968047	698	0.003898	1.064597
662	0.012676	0.967609	699	0.002846	1.072708
663	0.012903	0.967161	700	0.001757	1.08106
664	0.013131	0.966702			
665	0.013361	0.966233			
666	0.013591	0.965757			
667	0.013819	0.965294			
668	0.014042	0.964864			
669	0.014257	0.96449			
670	0.01446	0.964195			
671	0.014647	0.964			
672	0.014816	0.963929			
673	0.014963	0.964005			
674	0.015085	0.96425			
675	0.015178	0.964688			
676	0.015238	0.965343			
677	0.015262	0.966239			
678	0.015246	0.967402			
679	0.015187	0.968857			
680	0.015081	0.970629			
681	0.014923	0.972745			
682	0.014709	0.975232			
683	0.014436	0.978119			
684	0.014101	0.981426			
685	0.013703	0.985145			
686	0.013247	0.989259			
687	0.012735	0.993753			
688	0.012167	0.998612			
689	0.011548	1.003823			
690	0.010877	1.009373			
691	0.010158	1.015248			
692	0.009392	1.021438			

